

SPATIAL AND TEMPORAL CUSP STRUCTURES OBSERVED BY MULTIPLE SPACECRAFT AND GROUND BASED OBSERVATIONS

K. J. TRATTNER¹, S. A. FUSELIER¹, T. K. YEOMAN², C. CARLSON³, W. K. PETERSON⁴, A. KORTH⁵, H. REME⁶, J. A. SAUVAUD⁶ and N. DUBOULOZ⁷

¹*Lockheed-Martin Advanced Technology Center, Palo Alto CA 94304, USA*

E-mail: trattner@star.spasci.com;

²*Department of Physics and Astronomy, University of Leicester,
Leicester LE1 7RH, England;*

³*University of California, Berkeley CA 94724, USA;*

⁴*Laboratory for Atmospheric and Space Physics, University of Colorado,
Boulder CO 80309, USA;*

⁵*Max-Planck-Institut für Aeronomie, Katlenburg-Lindau Germany;*

⁶*CESR, Toulouse France;*

⁷*LPCE/CNES, Orleans France*

(Received 10 February 2003; Accepted 30 February 2004)

Abstract. Downward precipitating ions in the cusp regularly exhibit sudden changes in ion energy distributions, forming distinctive structures that can be used to study the temporal/spatial nature of reconnection at the magnetopause. When observed simultaneously with the Polar, FAST, and Interball satellites, such cusp structures revealed remarkably similar features. These similar features could be observed for up to several hours during stable solar wind conditions. Their similarities led to the conclusion that large-scale cusp structures are spatial structures related to global ionospheric convection patterns created by magnetic merging and not the result of temporal variations in reconnection parameters. The launch of the Cluster fleet allows cusp structures to be studied in great detail and during changing solar wind conditions using three spacecraft with identical plasma and field instrumentation. In addition, Cluster cusp measurements are linked with ionospheric convection cells by combining the satellite observations with SuperDARN radar observations that are used to derive the convection patterns in the ionosphere. The combination of satellite observations with ground-based observations during variable solar wind conditions shows that large-scale cusp structures can be either spatial or temporal. Cusp structures can be described as spatial features observed by satellites crossing into spatially separated flux tubes. Cusp structures can also be observed as poleward-traveling (temporal) features within the same convection cell, most probably caused by variations in the reconnection rate at the magnetopause.

Keywords: cusp geometry, cusp structures, precipitating ions

Abbreviations: APL – Applied Physics Laboratory, Johns Hopkins University; DMSP – Defense Meteorological Satellite Program; ML – magnetic local time; FAST – Fast Auroral SnapshoT satellite; SC – spacecraft

1. Introduction

Magnetic reconnection between the interplanetary magnetic field (IMF) and the geomagnetic field is most probably the dominant process whereby mass and energy are transferred from the solar wind into the magnetosphere. The classical picture of magnetic reconnection was presented by Dungey (1961), where a purely southward IMF and the northward geomagnetic field merged at the sub-solar magnetopause. Convincing evidence about magnetic reconnection has been accumulated with the observation of magnetosheath ions in the boundary layer inside the magnetopause (e.g., Paschmann et al., 1979; Sonnerup et al., 1981) and precipitating ions in the cusp (e.g., Escoubet et al., 1997; Reiff et al., 1977). The incoming magnetosheath distribution is truncated as it crosses the magnetopause so that only a limited part of the initial magnetosheath distribution enters the magnetosphere, forming a characteristic D-shaped distribution that had been predicted by Cowley (1982) and observed by, e.g., Fuselier et al. (1991, 2001). These ions will also stream continuously into the cusp along newly opened magnetic field lines (e.g., Lockwood and Smith, 1993, 1994; Onsager et al., 1993) and exhibit distinct energy versus latitude dispersion patterns as predicted by Rosenbauer et al. (1975) and observed by Shelley et al. (1976).

The complicated structures in cusp precipitation, with variations in flux levels and sudden changes in the energy of the precipitating ions (e.g., Newell and Meng, 1991; Escoubet et al., 1992), are the basis of a debate as to whether dayside reconnection is quasi-steady or transient (e.g., Newell and Sibeck, 1993; Lockwood et al., 1994; Trattner et al., 2002a, and the references therein). All newly opened magnetic field lines convect under the joint action of magnetic tension and momentum transfer from shocked solar wind flow. Thus transient cusp steps are convected, creating an ever-changing structural profile of precipitating cusp ions for observing satellites. This interpretation is based on a model by Cowley and Lockwood (1992) (for which the existence of cusp steps was predicted by Cowley et al. (1991) and Smith et al. (1992)). In this pulsating cusp model, cusp steps are the result of changes in the reconnection rate at the magnetopause that creates neighboring flux tubes in the cusp with different time histories since reconnection (e.g., Lockwood and Smith, 1994). While single-satellite observations are unable to demonstrate that steps in the cusp ion distribution signatures are moving, observations of steps have been interpreted as temporal rather than spatial variations. The observation of poleward moving events by the EISCAT radar (see Lockwood, 1995, 1996; Lockwood et al., 1995) is a natural consequence of a temporal feature, not predicted by a spatial interpretation, and supports this view.

The appearance of temporal cusp steps also depends on the satellite velocity relative to the convection velocity of the cusp structures. Satellites

crossing the boundary from a newly opened flux tube to an older one would encounter a decrease in the ion energy dispersion, while satellites crossing from an older flux tube into a recently opened newer one would see an increase in the ion energy signature. Figure 1 illustrates how one convecting cusp structure will be observed by a slow-moving high-altitude satellite like Polar (crossing the cusp in about 3 hours) and a fast-moving low-altitude satellite like FAST (crossing the cusp in 3 minutes). The slow-moving Polar spacecraft should be overtaken by the convecting structures and move from a “old” flux tube to a “newer” flux tube with less time since reconnection. As shown in Figure 1 (bottom panel), Polar will encounter an increase in the cusp ion energy dispersion. In contrast, the rapidly moving low-altitude FAST spacecraft would overtake the convecting cusp structure. FAST would cross from a “new” flux tube into an “older” one, encountering a decrease in the cusp ion energy dispersion (Figure 1, top panel). When observed on multiple satellites with large altitude separation in the cusp, structures caused by temporal variations of the reconnection rate should not only convect with the solar wind, but should also appear differently at different satellites.

Another characteristic to be considered in the observation of temporal structures in the cusp is the number of structures encountered by satellites at different altitudes like Polar and FAST. Depending on the convection speed of the reconnection pulses, the pulse frequency, and the spacecraft velocity in the cusp, many more pulses can be expected on Polar than on FAST.

Flux tubes on open field lines with precipitating magnetosheath ions could also be spatially separated, emanating from multiple X-lines. Crossing the boundary between such spatially separated flux tubes would also appear as a step in the ion energy dispersion due to the different time history since

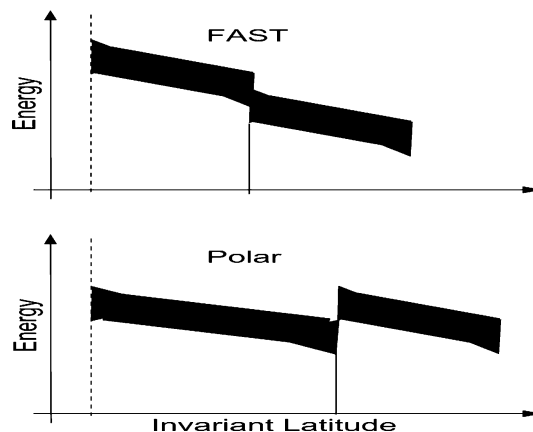


Figure 1. Schematic representation of one temporal step in the cusp ion energy dispersion as observed by satellites at vastly different altitudes, e.g., FAST and Polar (from Trattner et al., 2002a).

reconnection for field lines within the two flux tubes (Lockwood et al., 1995). However, this step would not be convecting with the solar wind but would appear as a standing feature in the cusp. Independent of the time delay between the cusp crossings or the satellite velocities, the satellites should encounter unchanged cusp structures at about the same latitude, observing a spatial feature. Such an observation would indicate that the reconnection rate at the magnetopause is rather stable, and not highly variable, to the point where it may even be zero for a limited period of time.

Figure 2 illustrates how two satellites encounter a spatial cusp structure (e.g., Trattner et al., 2002a). It also illustrates how this spatial feature might be encountered at slightly different latitudes by the two satellites. Spacecraft II enters flux tube I at lower latitudes than spacecraft I. The differences in the positions where the satellites enter the cusp are the simple consequence of the form of the equatorward edge of the cusp and the orbital paths of the satellites.

The latitudinal extent of individual cusp structures observed by two satellites also depends on the form of the flux tube and the orbital path intersecting it. These slight variations can, however, lead to misleading interpretations. Since temporal structures are expected to move with the convection flow, variations in the extent of structures could be interpreted as motion. The interpretation is especially difficult when spacecraft close together and at about the same altitude (e.g., Cluster) observe regular structures like the classical staircase.

The appearance of spatial structures has also been discussed by Wing et al. (2001), who modeled cusp precipitation characteristics for periods with a dominant B_y IMF. For these conditions they found that a characteristic “double cusp” signature was not only predicted but also observed in DMSP

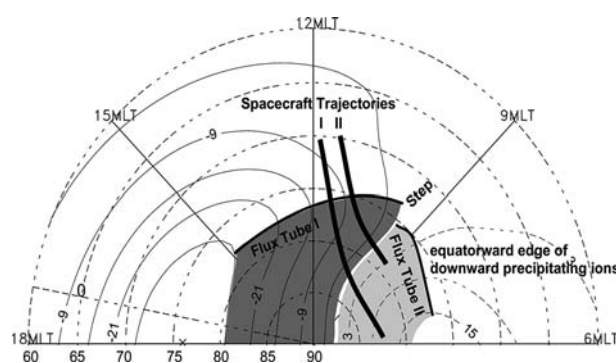


Figure 2. Ionospheric convection cells derived from the APL statistical model for $-B_z$ and $-B_y$ input. To illustrate how major cusp structures could be spatial instead of temporal, two flux tubes and two satellite trajectories have been superimposed on the plasma convection cells (from Trattner et al., 2002a).

satellite data. Also using multi-spacecraft observations, Onsager et al. (1995) showed two cusp crossings of the high-altitude Dynamic Explorer 1 (DE 1) and low-altitude DE 2 spacecraft separated by 20 minutes. A similar step in the ion dispersion signature at both spacecraft was interpreted as a spatial structure rather than a temporal variation of the reconnection rate. This event is especially interesting since the low-orbiting satellite encountered an upward step. A temporal convecting cusp structure would require the satellite to move along the open-closed field line boundary to allow the convecting structure to overtake the rapidly moving low-altitude satellite. However, the observing satellite was in a meridian orbit (i.e., presumably perpendicular to the open-closed field line boundary). Further evidence that cusp ion steps can be produced in steady state by spatial variations has also been discussed by, e.g., Newell and Meng (1991), Phillips et al. (1993), Lockwood and Smith (1994) and Weiss et al. (1995).

Ambiguity between spatial and temporal variations is a common problem in interpreting any sequence of data from an orbiting satellite. Multi-spacecraft observations have proven their usefulness in distinguishing between spatial and temporal phenomena. Ground-based information offers an opportunity for remote sensing of the plasma in a given region over a prolonged period. Such measurements also distinguish between temporal and spatial structures but suffer from lower resolution. In addition, transient signatures in the cusp observed from the ground by radar cannot unambiguously define the structures as being caused by precipitating ions (e.g., Lockwood et al., 1993).

In this study we review multi-spacecraft observations from Interball, FAST, Polar and three Cluster spacecraft. In addition, the Cluster observations are discussed in conjunction with SuperDARN radar observations. Among the strong evidence supporting the theory that cusp structures are spatial features, we also present evidence that structures observed within a flux tube appear to be temporal as discussed by Trattner et al. (2002a).

2. Mid- and high- altitude cusp observations

Trattner et al. (1999) compared cusp observations made by the toroidal imaging mass-angle spectrograph (TIMAS) on Polar (Shelley et al., 1995) with simultaneous observations made by the ION and HYPERBOLOID instruments on the Interball-AP spacecraft (Dubouloz et al., 1998; Sauvaud et al., 1998). Figure 3 shows a comparison of Polar/TIMAS proton flux data ($1/(\text{cm}^2 \text{ s sr keV/e})$) observed at an altitude of 5–6 R_E with Interball/ION, HYP observations at 3 R_E altitude for the cusp crossings on 3 May 1997, 13:30 to 15:10 UT. The data are plotted versus invariant latitude (ILAT). Both satellites crossed the cusp near local noon in opposite directions. Polar

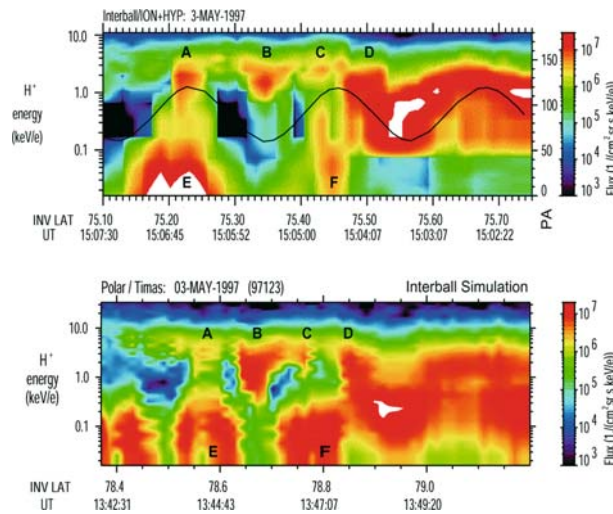


Figure 3. Comparison of flux measurements ($1/(\text{cm}^2 \text{ s sr keV/e})$) by Interball-AP/ION + HYP and Polar/TIMAS at the open-closed field line boundary for the 3 May 1997 cusp event. Polar/TIMAS observations were sampled to obtain a pitch angle distribution similar to Interball/ION. The cusp observations occurred at about the same local time but separated in time by 1 hour 25 minutes. The similarities in the ion dispersion signatures are interpreted as spatial structures rather than temporal variability in the reconnection rate (from Trattner et al., 1999).

was moving poleward and first encountered downward precipitating cusp ions at the equatorward edge of the cusp at about 13:40 UT, while Interball-AP was moving equatorward and left the cusp at about 15:06 UT.

The Interball-AP ION and HYPERBOLOID data are sampled during a two-minute spin period. This causes the pitch angle (PA) window to alternate between upgoing and downgoing ions within a two-minute spin (see black line in the top panel of Figure 3). The ION instrument encountered three sudden decreases in the low-energy cutoff of cusp ions close to the equatorward edge of the cusp. In Figure 3, the three steps are at 75.2° (A), 75.35° (B), and 75.45° (C) ILAT. The three downward steps are followed by a sharp drop of the ion energy at 75.5° (D) ILAT.

To compare Polar/TIMAS with Interball-AP ION and HYPERBOLOID under similar conditions, the two-minute pitch angle period was simulated with TIMAS data. The pitch angles observed at Interball during those steps and structures are transferred from Interball-AP to Polar latitudes, and only the same pitch angle ranges have been accumulated from the Polar measurements. The bottom panel in Figure 3 shows the TIMAS data as they would have been observed by ION and HYPERBOLOID on Interball-AP at the time that Polar crossed into the cusp. The data are averaged over 12 seconds (two spins) for the TIMAS energy range from 16 eV/e to 33 keV/e.

Polar encountered downward precipitating ions with energies up to 10 keV/e briefly at about 78° and 78.2° ILAT while crossing the ion open-closed field line boundary several times. It finally moved completely into the cusp and continuously measured downward precipitating ions at 13:42 UT. The energy of the downward precipitating ions remained constant until Polar reached 78.85° ILAT (13:47 UT), but included three short sudden decreases of the low-energy cutoff of cusp ions at 78.55° (A), 78.65° (B), and 78.75° (C) ILAT. At 78.85° (D) the downward precipitating cusp ion energy dropped from an average of about 5 keV/e to 200 eV/e.

The TIMAS and ION/HYPERBOLOID observations in the cusp are 1 hour 25 minutes apart but show remarkable similarities. In both observations there are three sudden drops of the low-energy cutoff (A, B and C) for ions, followed by a sharp decrease in the ion energy (D). The subsequent rise of ion energy in the ION data, caused by the slow movement of the pitch angle window, is also reproduced in the TIMAS data. The flux enhancements at lower energies (E and F) seen by both HYPERBOLOID and TIMAS are also well-reproduced. In addition, the changes in latitude between the steps are similar in both observations despite the overall latitude difference. The TIMAS and ION/HYPERBOLOID observations are close to the equatorward edge of the cusp; therefore, these observations represent flux tubes that have been recently opened. For the 3 May 1997 event, a series of distinctive features – three brief decreases in the low-energy cutoff followed by a step-down in ion energy – have moved about 3° equatorward and remained close to the equatorward edge of the cusp. These features were still observable after 1 hour 25 minutes, and appear to be spatial structures rather than temporal features caused by variations in the reconnection rate.

3. Low-and high-altitude observations

As outlined above, the comparison of cusp observations from satellites at different altitudes is helpful when distinguishing between temporal and spatial structures, since temporal structures would appear different at satellites at different altitudes. This technique has been successfully used by Onsager et al. (1995), Trattner et al. (2002a, b), and others. An extreme combination of cusp observations by satellites at different altitudes is achieved by combining FAST (at about 3000 km) with Polar (up to $8 R_E$) with their associated very different cusp crossing times of 3 minutes and 3 hours, respectively. Trattner et al. (2002a) compared major steps in the ion energy dispersion of four Polar-FAST cusp crossings during quiet solar wind and IMF conditions. This restriction was chosen to avoid changes in cusp structures due to changes in the location of the X-line at the magnetopause.

Figure 4 shows solar wind observations by the Solar Wind Experiment (SWE) and the Magnetic Field Investigation (MFI) onboard the Wind spacecraft for the Polar-FAST cusp crossings on 8 May 1998. The data have been propagated by about 38 minutes to account for the travel time from the Wind spacecraft to the magnetopause. Plotted are solar wind density N , solar wind velocity V_x and the magnetic field components B_x (thick line), B_y (thin line) and B_z (shaded area). Black bars indicate the times when Polar and FAST crossed the cusp and illustrate the temporal separation of the spacecraft. For this 6-hour interval the solar wind conditions were stable, with the solar wind density slightly decreasing from 3.5 cm^{-3} to 2.5 cm^{-3} and a solar wind velocity of about 600 km/s. The IMF observations indicate that B_z was southward for the entire interval, with an average of about -2 nT . B_y was the weakest component, with an average of about -1 nT , while B_x was the dominant component, with an average of about 4 nT .

A comparison of the flux measurements for the Polar and FAST cusp passes on 8 May 1998 is shown in Figure 5. The spacecraft crossed the cusp on field lines mapping to about 09:40 MLT (Polar) and 12:00 MLT (FAST), resulting in a temporal and spatial separation by up to 5 hours in UT and up to 3 hours in MLT. Plotted are H^+ flux measurements as observed by the Ion ElectroStatic Analyzer (IESA) (Carlson et al., 2001) (top) and TIMAS (bottom) instruments on FAST and Polar, respectively. White regions in the

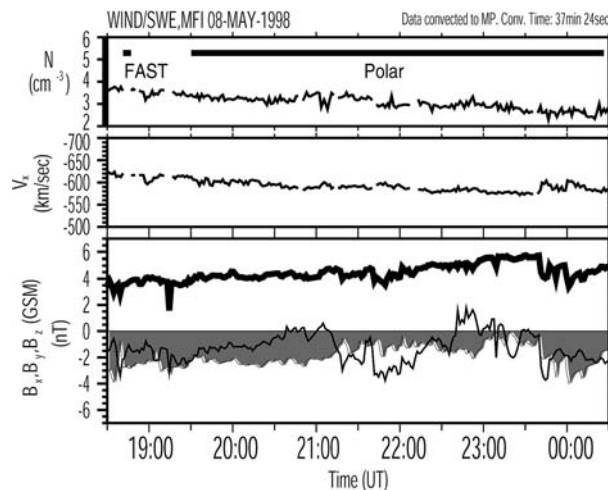


Figure 4. Solar wind parameter measurements by Wind/SWE, MFI upstream of the Earth's bow shock on 8 May 1998. The data have been propagated by about 38 minutes to account for the travel time from the Wind spacecraft to the magnetopause. Plotted are solar wind density N , solar wind velocity V_x and the magnetic field components B_x (thick line), B_y (thin line), and B_z (shaded area). Black bars indicate the times when Polar and FAST crossed the cusp to illustrate the temporal separation of the spacecraft (from Trattner et al., 2002a).

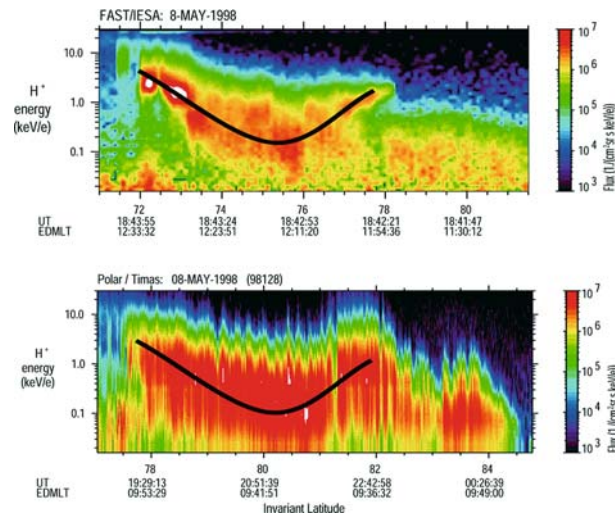


Figure 5. Comparison of FAST/IESA and Polar/TIMAS omnidirectional flux measurements ($1/(\text{cm}^2 \text{ s sr keV/e})$) for cusp crossings on 8 May 1998. The observations are separated by up to 3 hours in MLT and up to 5 hours in time. Even for these extreme spatial and temporal separations, there are remarkable similarities in the FAST/IESA and Polar/TIMAS cusp observations (from Trattner et al., 2002a).

color-coded plot indicate regions with flux levels above the maximum flux level indicated in the color bars. To help to guide the eye, additional lines have been overlaid which represent an average location of the maximum flux in the cusp ion energy dispersion. The FAST spacecraft, moving equatorward in this event, exited the cusp at about 18:44 UT at 72° ILAT and crossed the downward precipitating ion region in about 3 minutes. Seen from the equatorward edge of the cusp at 72° ILAT, the FAST cusp crossing is characterized by a classical velocity dispersion, with lower energy particles arriving at higher latitudes. This velocity filter effect (e.g., Rosenbauer et al., 1975; Onsager et al., 1993) is smoothly reversed at higher latitudes, where the energy of precipitating ions starts to increase again and forms a new maximum. After this second maximum at about 78° ILAT, the cusp ion energy decreases again, in agreement with the classical velocity dispersion.

The Polar spacecraft, moving poleward, encountered downward precipitating ions at about 19:15 UT at 77.5° ILAT. However, in contrast to the 3-minute snapshot of the cusp by FAST, Polar observed precipitating cusp ions for 5 hours. Nevertheless, Polar observed the same basic cusp structure seen by FAST. Cusp ion energies first decreased with increasing ILAT and smoothly reversed at about 80.5° ILAT, to form a new maximum at 82° ILAT. After the second maximum, the cusp ion energy continued to decrease again.

The Polar cusp pass also showed minor structures superimposed on the major cusp ion signature. There are periodic increases and decreases in the cusp ion energy, with a period of about 10 minutes. This feature could be the signature of surface waves at the magnetopause that push the X-line slightly in and out, thereby slightly changing the distance from the spacecraft to the X-line. This feature could also be the signature of pulsed reconnection. Lockwood (private communication, 2001) pointed out that for this specific example the ratio of Polar to FAST cusp steps encountered by the spacecraft should be about 20, which is indeed the case. The form and number of the cusp steps is in agreement with predictions from the pulsed reconnection model (e.g. Lockwood et al., 1998).

If cusp structures are spatial features, similar cusp structures should form for similar IMF conditions when observed in about the same MLT sector. This was the motivation for a subsequent study by Trattner et al. (2002b) who compared three Polar-FAST crossings observed at about the same MLT in the pre-noon sector and during very similar solar wind and IMF conditions.

Figure 6 shows solar wind observations made by Wind/SWE and Wind/MFI for the Polar and FAST cusp crossings on 22 October 1998. The data have been propagated by about 10 minutes to account for the travel time from the Wind spacecraft to the magnetopause. Plotted are solar wind

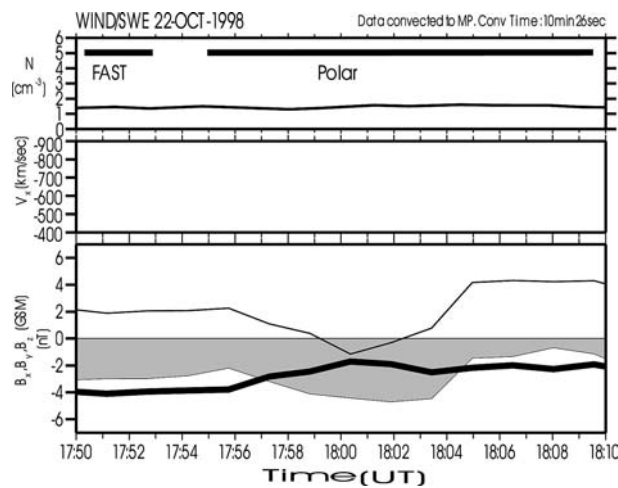


Figure 6. Solar wind parameter measurements by Wind/SWE, MFI upstream of the Earth's bow shock on Oct. 22, 1998. The data have been propagated by about 10 minutes to account for the travel time from the Wind spacecraft to the magnetopause. Plotted are solar wind density N , solar wind velocity V_x and the magnetic field components B_x (thick line), B_y (thin line) and B_z (shaded area). Black bars indicate the times when Polar and FAST crossed the cusp, illustrating the temporal separation of the spacecraft (from Trattner et al., 2002b).

density N , solar wind velocity V_x and the magnetic field components B_x (thick line), B_y (thin line) and B_z (shaded area). Black bars indicate the times when Polar and FAST crossed the cusp and illustrate the temporal separation of the spacecraft. The solar wind density and velocity were about 1.5 cm^{-3} and 600 km/s , respectively. The IMF observations indicate that B_z was southward for the entire interval, with an average value of about -3 nT , B_y was at about 3 nT with a brief negative period at 18:01 UT, and B_x was also negative with an average value of about -3 nT .

Polar and FAST crossed the cusp on 22 October 1998, in the morning sector at about 10:30 MLT (Polar) and 09:40 MLT (FAST), separated by up to 20 minutes in UT and by about 1 hour in MLT. The satellites again moved in opposite directions, with Polar moving equatorward and FAST moving poleward. A comparison of Polar and FAST flux measurements ($1/(\text{cm}^2 \text{ s sr keV/e})$) for the cusp crossings is shown in Figure 7. Plotted are H^+ flux measurements as observed by the IESA (top) and TIMAS (bottom) instruments on FAST and Polar, respectively. Also indicated in the Polar and FAST flux panels are the energies where the maximum flux of the cusp ions occurred. To guide the eye, additional lines have been overlaid to emphasize structures in the ion energy distribution.

Both spacecraft observed distinct energy-latitude dispersions typical for southward IMF with the highest energy ions arriving at the lowest ILAT

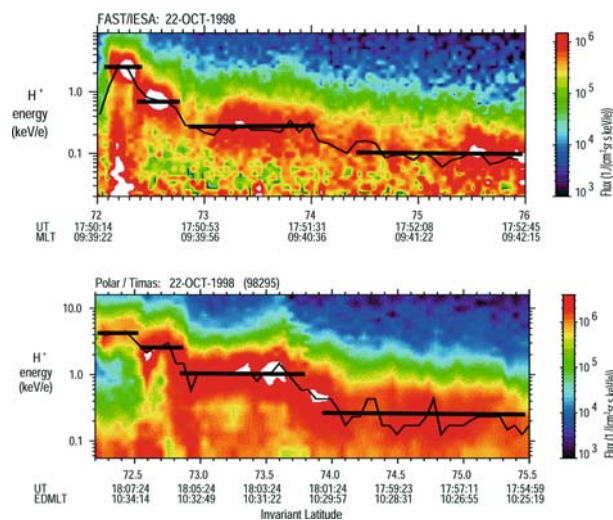


Figure 7. Comparison of FAST/IESA and Polar/TIMAS flux measurements ($1/(\text{cm}^2 \text{ s sr keV/e})$) for cusp crossings on 22 October 1998. The observations are separated by about 1 hour in MLT and 20 minutes in UT. The cusp structures in the ion dispersion signatures are interpreted as spatial rather than temporal structures (from Trattner et al., 2002b).

and lower-energy particles arriving at successively higher ILAT. In addition, these decreasing ion energy dispersions at both spacecraft were interrupted by three distinctive cusp steps. The FAST spacecraft entered the cusp at about 17:50 UT, crossed the downward precipitating ion region in 3 minutes, and moved onto lobe field lines. The FAST cusp crossing shows three major steps in the ion energy dispersions that are located at 72.3° , 73° , and 74.2° ILAT. The cusp ion energy decreased sharply from about 3 keV to 700 eV and subsequently to 300 eV for the first two steps. These two cusp steps are followed by a smoother decrease of the cusp ion energy to about 100 eV.

The Polar spacecraft crossed the cusp in about 20 minutes and left the precipitating ion region at 18:10 UT, 20 minutes later than FAST. In agreement with the cusp structures observed by FAST, the decreasing ion energy dispersion seen by Polar is interrupted by three steps located at 72.6° , 72.9° , and 73.8° ILAT. As in the FAST cusp observations, the first two steps seen by Polar show sharp decreases of the cusp ion energy from 4 keV to about 1.5 keV and subsequently to 1 keV. These are followed by a smoother decrease to about 200 eV. Comparing the Polar observations with FAST observations, we find that, while the spacecraft encounter cusp steps at slightly different latitudes, they have not moved within the cusp. This is in agreement with a spatial interpretation of cusp structures. The differences in the cusp ion energies can be attributed to the separation in local time of the two spacecraft and the subsequent different locations where the spacecraft entered neighboring flux tubes with their independent time history since reconnection. The cusp ion energy is also influenced by the location of the X-line and the degree of acceleration of the ions as they cross the dayside magnetopause (e.g., Lockwood and Smith, 1992).

By comparing the Polar and FAST cusp crossings, there is no indication that Polar observed a different number of major cusp steps than FAST did, as we would expect for temporal structures. There is also no indication that FAST encountered a “step-down” in the ion energy dispersion signature while Polar encountered a “step-up”, which is also expected for the observations of temporal structures by spacecraft with large altitude separations. Both spacecraft observed the same number and orientation of cusp structures that also have not moved (convected) relative to each other, as expected for temporal cusp features. In addition, Trattner et al. (2002b) showed that all three events observed at about the same MLT in the pre-noon sector and during similar stable solar wind and IMF conditions had the same sequence of cusp steps, two sharp drops in the ion energy dispersion followed by a smoother transition to another energy level. Cusp structures appear to be not only spatial events but seem to be organized in the same sequence for similar IMF conditions.

4. Spatial cusp structures observed by cluster and radar observations

Studies like Trattner et al. (2002a) have been limited to events during stable solar wind and IMF conditions to ensure that changes in the cusp ion energy dispersion are not caused by changes in the location of the X-line. In a study by Trattner et al. (2003), multi-spacecraft observations from three Cluster spacecraft are combined with SuperDARN radar observations to investigate cusp structures in unprecedented detail and under any solar wind and IMF conditions.

Figure 8 shows solar wind conditions for the Cluster cusp crossing on 25 July 2001, observed by the Wind/SWE and MFI instruments. The solar wind data have been propagated by about 8 minutes to account for the travel time from the Wind spacecraft to the magnetopause. Solar wind density N and velocity V_x for July 25, 2001, were about 4 cm^{-3} (top panel) and about 560 km/s (middle panel), respectively. The IMF components B_x (black line), B_y (green line) and B_z (colored area) are shown in the bottom panel. At the beginning of the Cluster cusp crossing until about 23:40 UT the IMF shows a typical Parker spiral configuration with a positive B_x of about 3 nT, a negative B_y of about -4 nT and a negative B_z of also about -4 nT (blue colored area). Starting at about 23:35 UT the B_z component rotated through zero (at 23:47 UT) and then switched northward to about 4 nT (red colored area). The B_y component changed direction from negative to positive for 15 minutes at about the same time that the B_z component changed from southward

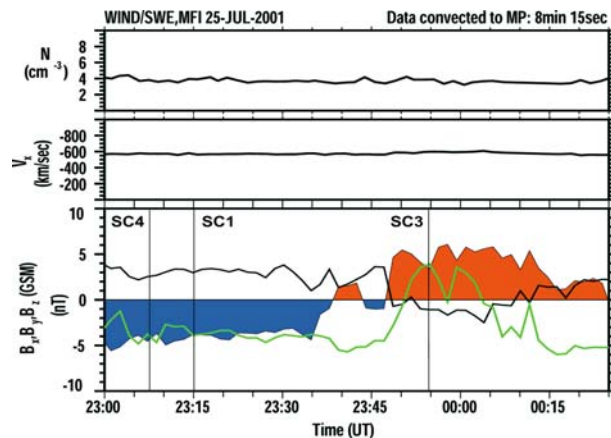


Figure 8. Solar wind parameter measurements by Wind/SWE, MFI on 25 July 2001. The data have been propagated by about 8 minutes to account for the travel time from the Wind spacecraft to the magnetopause. Plotted are solar wind density N , solar wind velocity V_x , and the magnetic field components B_x (black line), B_y (green line) and B_z (shaded area). Black lines indicate the times when Cluster satellites crossed into the cusp to illustrate the temporal separation of the spacecraft (from Trattner et al., 2003).

to northward. Finally, the B_x component also switched from positive to negative for about 15 minutes. Black lines indicate the times when the Cluster satellites crossed into the cusp to illustrate the temporal separation of the spacecraft. SC4 and SC1 entered the cusp at 23:09 UT and 23:15 UT, respectively, during which time the IMF was southward and stable for an extended period of time. SC3 entered the cusp at 23:54 UT, 7 minutes after the IMF switch northward.

Figure 9 shows the temporal separation of the Cluster/CIS observation for the cusp crossings on 25 July 2001. Plotted are H^+ omnidirectional flux measurements ($1/(\text{cm}^2 \text{ s sr keV/e})$) from SC1 (top panel), SC3 (middle panel) and SC4 (bottom panel), observed in an MLT range from 14:00 to 11:00, an ILAT range from 76.8° to 86° , and a geocentric distance from 4.8 to $6 R_E$. White regions in the color-coded plot indicate regions with flux levels above the maximum flux level indicated in the color bars.

SC1 entered the cusp at about 23:15 UT, marked by a white line (1a), where it encountered downward precipitating magnetosheath ions. SC1 subsequently observed the typical cusp ion energy dispersion for a southward interplanetary magnetic field, with lower energy ions arriving at higher latitudes. The ion energy distribution decreases smoothly, indicating a constant magnetospheric reconnection rate at the magnetopause. At about 23:37 UT, SC1 encounters a sudden increase in the ion energy dispersion (1c), consistent with a typical step-up ion signature for crossing onto magnetic field lines that have been reconnected more recently. The ion energy of the precipitating ions again decreases until about 23:45 UT, when a new low is reached. Pitch angle

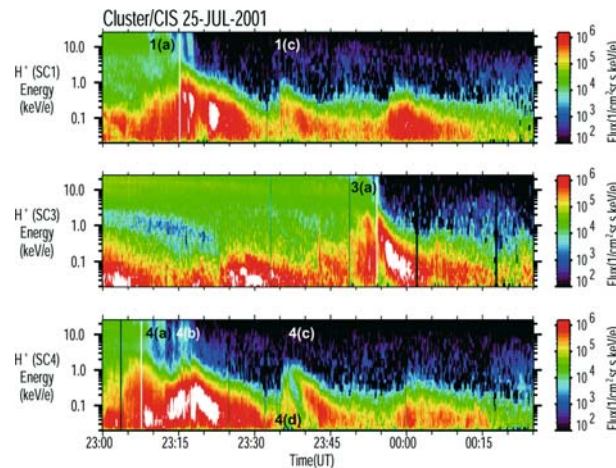


Figure 9. Cluster/CIS observation for cusp crossings on 25 July 2001. Plotted are H^+ omnidirectional flux measurements ($1/(\text{cm}^2 \text{ s sr keV/e})$) for SC1, SC3 and SC4. All satellites encounter distinctive structures, sudden jumps in the ion energy dispersion that are similar on SC1 and SC4, but different on the later arriving SC3 satellite (from Trattner et al., 2003).

analysis of this low energy distribution shows that it is solely composed of ionospheric ion outflow.

SC3 crosses into the cusp at 23:54 UT, indicated by a white line in the color spectrogram (3a). This spacecraft also observes a typical decreasing ion energy dispersion for a stable rate of reconnection with no further cusp structures later on. The fact that the observed ion dispersion at SC3 is typical for a southward IMF configuration while the IMF changed northward 6 minutes earlier is the result of a delayed response of the magnetosphere to changes in the solar wind. A delayed response to IMF changes is not unusual and is also observed in the ionospheric convection patterns that are significantly reconfigured about 10 minutes after the IMF change.

The first Cluster satellite to enter the cusp on 25 July 2001 is SC4 at 23:09 UT (4a). The cusp encounter is followed by a decreasing ion energy dispersion which is reversed at about 23:13 UT. The precipitating ion energy reaches a new maximum at 23:15 UT (4b), the same time that SC1 enters the cusp. This enhancement is explained by a change in the configuration of the convection cell which brought the ion open-closed field line boundary closer to the position of SC4, shortening the convection distance (see Trattner et al., 2003). The ion energy again starts to decrease before a second brief increase at 23:35 UT. A detailed pitch angle analysis showed that this signature was caused by ionospheric outflow and not ion precipitation from the magnetosheath. A pitch angle analysis of the proton distribution for the same time interval revealed that such a localized ion outflow distribution was also present at the position of SC1. However, this population was not as clearly separated from the immediately following downward precipitating ions as at the location of SC4. SC4 encounters this second sudden increase in ion energy at about 23:37 UT (4c), which is similar to the increase observed by SC1 at the same time. This step-up structure is also followed by a decrease of ion energy until about 23:45 UT, where a constant low energy flux is reached, typical for high latitude ionospheric outflow.

Figure 10 shows a combination of the temporal and spatial separations of the Cluster spacecraft. The Cluster magnetic foot points and the ionospheric convection streamlines for 25 July 2001, at 23:37 UT, are shown. The ionospheric convection streamlines, presented as contour lines, have been calculated using line-of-sight velocity data from the 8 operating northern hemisphere SuperDARN radars (Greenwald et al., 1995) together with the technique of Ruohoniemi and Baker (1998). Here the fit to the line-of-sight data is made to a sixth spherical harmonic expansion, with the fit stabilized by a statistical pattern keyed to the upstream IMF data from the Wind satellite, delayed by 8 minutes to allow for the propagation time from the spacecraft to the magnetopause (Ruohoniemi and Greenwald, 1996).

Overlaid on the magnetic foot points are 14-minute intervals of the Cluster/CIS flux measurements presented in Figure 9, which are centered on

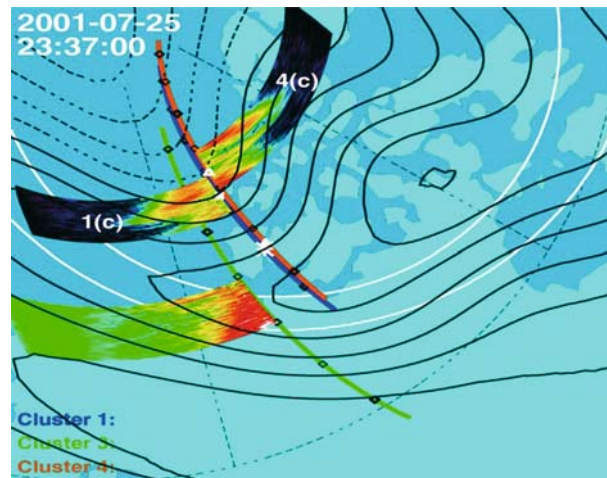


Figure 10. Composite plot of Cluster magnetic foot points and ionospheric convection streamlines for 25 July 2001, at 23:37 UT. Overlaid on the magnetic foot points are 14-minute intervals of the Cluster/CIS flux measurements presented in Figure 9, which are centered on the actual position of the Cluster satellites at 23:37 UT. The original entry points of SC1 and SC4 into the cusp are marked with a star and a triangle, respectively, along the tracks of their magnetic foot points. SC1 and SC4 are deep inside the cusp and have just entered the dawn convection cell (dashed lines) resulting in an almost simultaneous sudden increase of the ion energy dispersion on both satellites (also marked with symbols), as expected from a spatial interpretation of cusp structures. During that time SC3 was still on closed field lines (from Trattner et al., 2003).

the actual position of the Cluster satellites at 23:37 UT. This representation shows the actual Cluster measurements in time at the proper spatial location. White lines in Figure 10 represent the average location of the auroral oval.

SC1 and SC4 are deep inside the cusp while SC3 is still on closed field lines. The original entry point of SC1 and SC4 into the cusp are marked with a star and a triangle, respectively, along the tracks of their magnetic foot points. At 23:37 UT the IMF shows a strong decrease in the value of B_z , which later changes sign. An equatorward directed bulge in the convection pattern moved rapidly equatorward which in turn allowed the dawn convection cell (dashed black lines) to move equatorward as well. At 23:37 UT, SC1 and SC4 have progressed poleward far enough to be overtaken by the equatorward moving dawn convection cell. The transfer from one convection cell to another resulted in an almost simultaneous sudden increase of the ion energy dispersion (structures 1c and 4c in Figure 9) on both satellites, indicating that the ion open-closed field line boundary in the dawn convection cell is much closer to the SC1 and SC4 magnetic footprints than in the dusk convection cell (solid black lines). The satellite positions at 23:37 UT, which are also the positions of the sudden increase in the ion energy dispersion, are marked with star (SC1) and triangle (SC4) symbols.

The sudden increase in the ion energy dispersion coincides with a satellite moving into a neighboring spatially separated flux tube (or convection cell). This feature was discussed above, based on earlier cusp observations by Trattner et al. (2002a, 2002b) during stable solar wind conditions. Figure 10 shows not only that such a scenario can take place but that it also occurs during dynamic solar wind IMF conditions. The change in IMF conditions most probably caused a change in the location of the reconnection site, which in turn caused a shift in the positions of spatially separated flux tubes.

5. Temporal cusp structures observed by cluster

Figure 11 shows solar wind conditions for the Cluster cusp crossing on 23 September 2001, observed by Wind/SWE, MFI. The solar wind data have been propagated by about 18 minutes to account for the travel time from the Wind spacecraft to the magnetopause. Figure 11 has the same format as Figure 8 and shows a highly variable solar wind density N covering a range between 5 and 20 cm^{-3} (top panel) and a solar wind velocity V_x of about 520 km/s (middle panel). The IMF components B_x (black line), B_y (green line) and B_z (colored area) are shown in the bottom panel. For the Cluster cusp crossing from 11:00 UT to 12:30 UT, the IMF is dominated by a strong

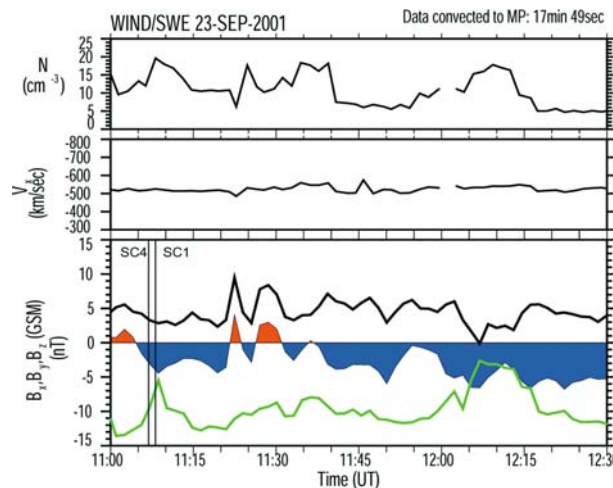


Figure 11. Solar wind parameter measurements by Wind/SWE, MFI on 23 September 2001. The data have been propagated by about 18 minutes to account for the travel time from the Wind spacecraft to the magnetopause. Plotted are solar wind density N , solar wind velocity V_x , and the magnetic field components B_x (black line), B_y (green line) and B_z (shaded area). Thin vertical black lines indicate the times when Cluster SC1 and SC4 satellites crossed into the cusp.

but variable negative B_y component ranging from -3 to -15 nT. The B_x component is positive and centered on 5 nT, while the B_z component is less than 5 nT and switches several times between northward (red) and southward (blue). This Cluster cusp event is characterized by strong variations in solar wind density and IMF directions that will introduce temporal changes in the reconnection location and, most probably, temporal changes in the reconnection rate. Black vertical lines indicate the times when the Cluster SC1 and SC4 satellites crossed into the cusp.

Figure 12 shows H^+ omnidirectional flux measurements ($1/(\text{cm}^2 \text{ s sr keV/e})$) from SC1 (top panel) and SC4 (bottom panel) for this cusp crossing. These measurements were observed in an MLT range from 11:30 to 13:00, an ILAT range from 75° to 83° and a geocentric distance from $4.5 R_E$ to $5.4 R_E$.

SC1 enters the cusp at about 11:08 UT, marked by a black vertical line. SC1 subsequently observes two typical step-up cusp structures in the ion energy dispersion at about 11:18 UT (1a) and 11:25 UT (1b). Cluster spacecraft SC4 enters the cusp about 1 minute before SC1 at 11:07 UT, also indicated by a black vertical line. Like SC1, SC4 encounters two step-up cusp structures at about 11:19 (4a) and 11:27 UT (4b). The two cusp steps at SC1 and SC4 are very similar to the spatial structures discussed before. However, their projection into the ionosphere revealed the temporal nature of these structures.

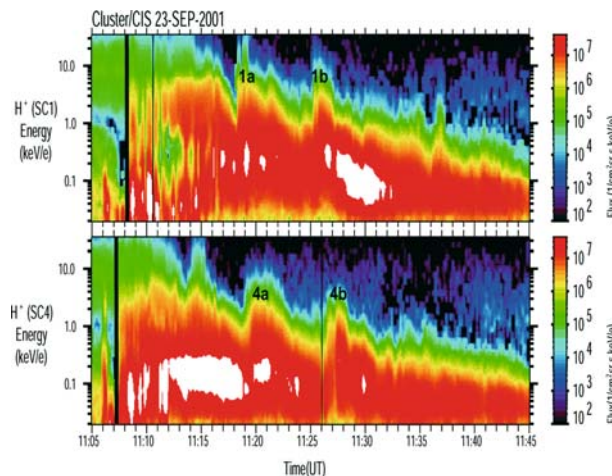


Figure 12. Cluster/CIS observation for a cusp crossing on 23 September 2001. Plotted are H^+ omnidirectional flux measurements ($1/(\text{cm}^2 \text{ s sr keV/e})$) for SC1 and SC4. The satellites encounter distinctive “step-up” structures in the ion energy dispersion that are similar on the two Cluster spacecraft. After comparing the satellite observations with simultaneous SuperDARN radar observations, these structures have been identified as temporal structures that are convecting poleward with the convecting magnetic field lines.

Figure 13 shows a composite plot to combine the temporal and spatial separations of the Cluster observations. Shown are the Cluster magnetic foot points and the ionospheric convection streamlines for 23 September 2001, at about 11:18 UT. Overlaid on the magnetic foot points are 14-minute intervals of the Cluster/CIS flux measurements presented in Figure 12, which are centered on the actual position of the Cluster satellites at 11:18 UT. The spacecraft are located at the intersection of the magnetic foot points with the white lines in the overlaid color spectrograms. Poleward (top) of the white lines, the “future” spectra to be observed by SC1 and SC4 are shown, while equatorward (bottom) of the white lines the spectra from the “past” are plotted.

SC1 and SC4 are deep inside the cusp and moving obliquely to the ionospheric convection direction while SC3 is still on closed field lines. The original entry points of SC1 and SC4 into the cusp are marked with a star and a triangle along the tracks of their magnetic foot points. In addition, a black dashed line marks the likely location of the ion open-closed field line boundary that intersects the cusp entry points. At 11:18 UT, SC1 encountered the first step-up cusp structure (1a). SC4, positioned just downstream and poleward of SC1

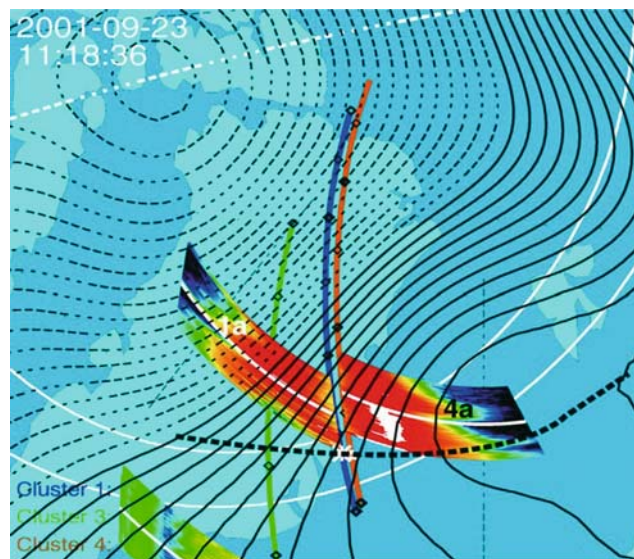


Figure 13. Composite plot of Cluster magnetic foot points and ionospheric convection streamlines for 23 September 23 2001, at 11:18 UT. Overlaid on the magnetic foot points are 14-minute intervals of the Cluster/CIS flux measurements presented in Figure 12, which are centered on the actual position of the Cluster satellites at 11:18 UT (indicated by white lines in the spectra). The original entry points of SC1 and SC4 into the cusp are marked with a star and a triangle, respectively, along the tracks of their magnetic foot points. Passing through this location is a thick dashed line representing the most likely position of the ion open-closed field line boundary. SC1 has just encountered a step-up cusp structure while along the convection path about 1° poleward of SC1, SC4 will encounter a similar step about 1 minute later.

along the convection path, will encounter a similar step marked (4a) in about 1 minute. Observing a similar step feature about 1° higher in latitude and about 1 minute later than the low latitude satellite is consistent with a temporal moving structure as predicted by the pulsed reconnection line.

The scenario repeats itself for the second step-up structure. Figure 14 shows the same composite plot as Figure 13 but 7 minutes later. At that time, SC1 encountered the second step-up cusp structure (1b), while again SC4, positioned just downstream and poleward of SC1, will encounter a similar step marked (4b) in about 1 minute and 1° higher in latitude. Also still visible in the 14-minute overlaid spectra for SC4 is the first step-up (4a). Both step structures observed by one spacecraft seem to have convected 1° poleward in the direction of the convection path within about 1 minute, which represents a convection velocity of about 1.5 km/s, in agreement with observed convection speed in the ionosphere of about 1.2 km/s, as measured by the SuperDARN radars (see also Lockwood et al., 1990, Pinnock et al., 1993). These poleward moving structures are consistent with temporal moving structures and could be an indication of a variation of the reconnection rate.

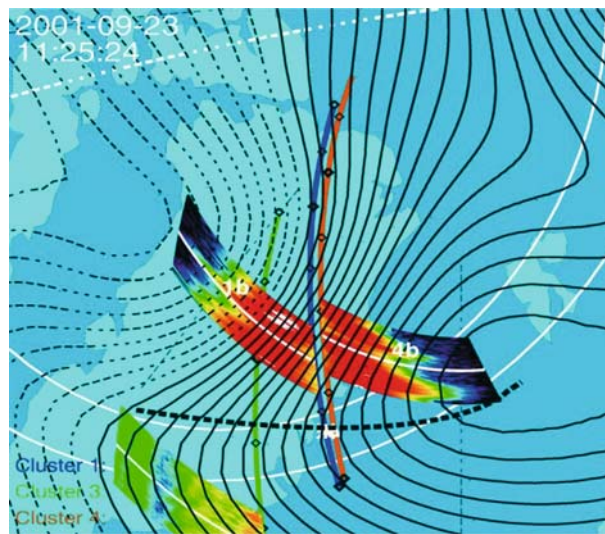


Figure 14. Composite plot of Cluster magnetic foot points and ionospheric convection streamlines for 23 September 2001, at 11:25 UT. Overlaid on the magnetic foot points are 14-minute intervals of the Cluster/CIS flux measurements presented in Figure 12, which are centered on the actual position of the Cluster satellites at 11:25 UT (indicated by white lines in the spectra). The original entry point of SC1 and SC4 into the cusp are marked with a star and a triangle, respectively, along the tracks of their magnetic foot points. Passing through this location is a thick dashed line representing the most likely position of the ion open-closed field line boundary. SC1 again encountered a step-up cusp structure while along the convection path about 1° poleward of SC1, SC4 will encounter a similar step about 1 minute later. The previous step-up structure is also still visible in the overlaid spectrogram of SC4.

6. Summary and conclusions

The spatial and temporal variations of the cusp reflect the spatial and temporal variations in dayside reconnection location and rate. Early on, sudden changes (steps) in the ion energy spectra were observed by various satellites. The nature of these steps in cusp ion energy dispersion has been discussed for more than a decade and evidence has been accumulated for two different mechanisms – temporal variations in the reconnection rate (i.e., pulsed reconnections) and spatial variations in the reconnection location.

In the pulsed cusp model, steps are described as periods of little or no reconnection at the magnetopause (e.g., Lockwood and Smith, 1989, 1990, 1994; Lockwood et al., 1998). These variations in the reconnection rate create a series of poleward convecting magnetic flux tubes (pulses) with different time histories since reconnection.

Spatial cusp structures have been studied by Onsager et al. (1995), Trattner et al. (2002a) and others, using observations from multiple satellites. These studies revealed that, while individual cusp crossings for different solar wind conditions are very dissimilar, cusp crossings by two satellites during stable solar wind conditions are remarkably similar over extended time periods (up to 5 hours) and spatial separations (about 2 hours in MLT) of the satellites. If this conclusion is correct, then reconnection at the magnetopause would be a rather constant process with only minor variations. Smaller cusp structures embedded in major steps most probably caused by such minor reconnection rate variations have been reported (Trattner et al., 2002a). Even changes in the IMF conditions, which move reconnection lines to different positions at the magnetopause and also move flux tubes emanating from these reconnection lines, exhibit spatial cusp structures (Trattner et al., 2003). While flux tubes would change their positions, cusp steps will still be encountered by crossing the boundary between the flux tubes, crossing onto open field lines with a different time since reconnection.

Recent observations made by the three Cluster spacecraft combined with simultaneous observations made by the SuperDARN radar network have allowed cusp structures to be investigated in unprecedented detail. This study revealed that, indeed, both spatial and temporal structures occur in the cusp. Our conclusions about the mechanisms to create temporal and spatial structures are:

- (1) Cusp structures are the result of temporal changes in the location of convection pattern that either drastically shorten or lengthen the convection length of magnetic field lines from the ion open-closed field line boundary to the position where they are intercepted by the satellites. The change can be a smooth reversal of a previous ion energy dispersion or a sudden step.

- (2) Cusp structures are caused by the entry into a different convection cell or flux tube where the location of the ion open-closed field line boundary was significantly different from that in the old cell. This can result in a step-up or step-down ion energy dispersion. The observed cusp structure is a spatial structure and will appear unchanged for satellites at every altitude (Trattner et al., 2002a, 2002b).
- (3) Cusp structures are caused by a variation of the reconnection rate at the reconnection location. This temporal cusp structure will be convected with the open geomagnetic field lines and travel along the ionospheric convection direction. In agreement with the pulsating cusp model (e.g., Lockwood and Smith, 1989), fast low-altitude satellites overtaking the convecting structure encounter a step-down ion energy dispersion while slow high-altitude satellites are overtaken by the convecting cusp structure and encounter a step-up dispersion profile.

While spatial and temporal processes have been observed, the combination of multi-spacecraft observations with large scale ground observations will allow new insight into pulse frequency, convection velocity, the magnitude of cusp steps, and the conditions necessary to observe either spatial or temporal cusp structures.

Acknowledgements

We acknowledge the use of ISTP K_p database. Solar wind observations were provided by K. Ogilvie at NASA/GSFC (Wind/SWE) and D.J. McComas (ACE/SWE). Observations of the interplanetary magnetic field were provided by R. Lepping at NASA/GSFC (Wind/MFI) and N. Ness (ACE/MFI). The work at Lockheed Martin was supported by NASA contracts NAS5-30302, NAG5-3596 and NAG5-13218. The work at the Max-Planck-Institut fuer Aeronomie was supported by DLR under contract 50 OC 8904 0 (Cluster-CIS). We would like to thank the SyperDARN PIs (W. A. Bristow, P. Dyson, R. A. Greenwald, T. Kikuchi, M. Lester, M. Pinnock, N. Sato, G. Sofko, J.-P. Villain, and A. D. M. Walker) for providing the coordinated cluster support radar modes which were running during the Cluster-SuperDARN spacecraft conjunctions.

References

- Carlson, C. W., McFadden, J. P., Turin, P., Curtis, D. W., and Magoncelli, A.: 2001. 'The Electron and Ion Plasma Experiments for FAST', *Space Sci. Rev.* **98**, 1.
- Cowley, S. W. H.: 1982. 'The Cause of Convection in the Earth's Magnetosphere: A Review of Developments During the IMS', *em Rev. Geophys. Res.* **20**, 531.

- Cowley, S. W. H., Freeman, M.P., Lockwood, M., and Smith, M.F.: 1991. 'The Ionospheric Signatures of Flux Transfer Events', in C.I. Barron (ed.), *CLUSTER: Dayside Polar Cusp*, European Space Agency Spec. Publ., ESA, pp. 105SP-330.
- Cowley, S. W. H., and Lockwood, M.: 1992. 'Excitation and Decay of Solar Driven Flows in the Magnetosphere-Ionosphere System', *Ann. Geophys.* **10**, 103.
- Dubouloz, N., Berthelier, J. -J., Malingre, M., Girard, L., Galperin, Y., Covinhes, J., Chugunin, D., Godefroy, M., Gogly, G., Guérin, C., Illiano, J. -M., Kossa, P., Leblanc, F., Legoff, F., Mularchik, T., Paris, J., Stzepourginski, W., Vivat, F., and Zinin, L.: 1998. 'Thermal Ion Measurements on Board Interball Aurora Probe by the Hyperboloid Experiment', *Ann. Geophys.* **16**, 1070.
- Dungey, J. W.: 1961. 'Interplanetary Magnetic Field and Auroral Zones', *Phys. Rev. Lett.* **6**, 47.
- Escoubet, C. P., Smith, M. F., Fung, S. F., Anderson, P. C., Hoffman, R. A., Baasinska, E. M., and Bosqued, J. M.: 1992. 'Staircase Ion Signature in the Polar Cusp: A Case Study', *Geophys. Res. Lett.* **19**, 1735.
- Escoubet, C. P., Bosqued, J. M., Hoffman, R. A., Berthelier, A., and Anderson, P. C.: 1997. 'Opposite Ion Dispersions Observed Quasi-simultaneously in the Polar Cusp by the DE-2 and Aureol-3 Satellites', *Geophys. Res. Lett.* **24**, 2487.
- Fuselier, S. A., Klumpar, D. M., and Shelley, E. G.: 1991. 'Ion Reflection and Transmissions During Reconnection at the Earth's Subsolar Magnetopause', *Geophys. Res. Lett.* **18**, 139.
- Fuselier, S.A., Waite, J.H., Avanov, L.A., Smirnov, V.M., Vaisberg, O.L., Siscoe, G. and Russell, C.T.: (2001). Characteristics of Magnetosheath Plasma in the Vicinity of the High Latitude Cusp. *J. Geophys. Res.*, submitted.
- Greenwald, R. A., Hunsaker, R. D., Sofko, G., Koehler, J., Nielsen, E., Pellinen, R., Walker, A. D. M., Sato, N., and Yamagishi, H.: 1995 'DARN/SUPERDARN A Global View of the Dynamics of High-latitude ConvectionSpace Sci. Rev. **71**, 761.
- Lockwood, M.: 1995. Ground-based and Satellite Observations of the Cusp: Evidence for Pulsed Magnetopause Reconnection, in P. Song, B. U. O. Sonnerup, and M. F. Thomsen (eds.), *Physics of the Magnetopause*, Geophys. Monogr. Ser., 90 AGU, Washington, D.C., pp. 417.
- Lockwood, M.: 1996. 'The Case for Transient Magnetopause Reconnection', *EOS Trans. AGU* **77**, 246.
- Lockwood, M., Cowley, S. W. H., Sandholt, P. E., and Lepping, R. P.: 1990. 'The ionospheric signatures of flux transfer events and solar wind dynamic pressure changes', *J. Geophys. Res.* **95**, 17113.
- Lockwood, M., Cowley, S. W. H., and Smith, M. F.: 1994. 'Comment on: 'By Fluctuations in the Magnetosheath and Azimuthal Flow Velocity Transient in the Dayside Ionosphere' by Newell and Sibeck', *Geophys. Res. Lett.* **21**, 1819.
- Lockwood, M., Davis, C. J., Smith, M. F., Onsager, T. G., and Denig, W. F.: 1995. 'Location and Characteristics of the Reconnection X-line Deduced from Low-altitude Satellite and Ground-based Observations, Defense Meteorological Satellite Program and European Incoherent Scatter data', *J. Geophys. Res.* **100**, 21803.
- Lockwood, M., Davis, C. J., Onsager, T. G., and Scudder, J. D.: 1998. 'Modeling Signatures of Pulsed Magnetopause Reconnection in Cusp Ion Dispersion Signatures Seen at Middle Altitudes', *Geophys. Res. Lett.* **25**, 591.
- Lockwood, M., Denig, W. F., Farmer, A. D., Davda, V. N., Cowley, S. W. H., and Lühr, H.: 1993. 'Ionospheric Signatures of Pulsed Reconnection at the Earth's Magnetopause', *Nature* **361**, 424.
- Lockwood, M. and Smith, M. F.: 1989. 'Low-altitude Signatures of the Cusp and Flux Transfer Events', *Geophys. Res. Lett.* **16**, 879.

- Lockwood, M., and Smith, M. F.: 1990. 'Reply to Comment by P.T. Newell on 'Low-altitude Signatures of the Cusp and Flux Transfer Events' by M. Lockwood and M.F. Smith', *Geophys. Res. Lett.* **17**, 305.
- Lockwood, M., and Smith, M. F.: 1992. 'The Variation of Reconnection Rate at the Dayside Magnetopause and Cusp Ion Precipitation', *J. Geophys. Res.* **97**, 14841.
- Lockwood, M., and Smith, M. F.: 1993. 'Comment on "Mapping the Dayside Ionosphere to the Magnetosphere According to Particle Precipitation Characteristics" by P.T. Newell and C.-I. Meng', *Geophys. Res. Lett.* **20**, 1739.
- Lockwood, M., and Smith, M. F.: 1994. 'Low- and Mid-altitude Cusp Particle Signatures for General Magnetopause Reconnection Rate Variations I Theory', *J. Geophys. Res.* **99**, 8531.
- Newell, P. T., and Meng, C.-I.: 1991. 'Ion Acceleration at the Equatorward Edge of the Cusp: Low-altitude Observations of Patchy Merging', *Geophys. Res. Lett.* **18**, 1829.
- Newell, P. T., and Sibeck, D. G.: 1993. 'Upper Limits on the Contribution of FTE's to Ionospheric Convection', *Geophys. Res. Lett.* **20**, 2829.
- Onsager, T. G., Kletzing, C. A., Austin, J. B., and MacKiernan, H.: 1993. 'Model of Magnetosheath Plasma in the Magnetosphere: Cusp and Mantle Particles at Low Altitudes', *Geophys. Res. Lett.* **20**, 479.
- Onsager, T. G., Chang, S.-W., Perez, J. D., Austin, J. B., and Jano, L. X.: 1995. 'Low-altitude Observations and Modeling of Quasi-steady Magnetopause Reconnection', *J. Geophys. Res.* **100**, 11831.
- Paschmann, G., Sonnerup, B.U.Ö., Papamastorakis, I., Scopke, N., Haerendel, G., Bame, S. J., Asbridge, J. R., Gosling, J. T., Russell, C. T., and Elphic, R. C.: 1979. 'Plasma Acceleration at the Earth's magnetopause: Evidence for Magnetic Field Reconnection', *Nature* **282**, 243.
- Phillips, J. L., Bame, S. J., Elphic, R. C., Gosling, J. T., Thomson, M. F., and Onsager, T. G.: 1993. 'Well-resolved Observations by ISEE 2 of Ion Dispersion in the Magnetospheric Cusp', *J. Geophys. Res.* **98**, 13429.
- Pinnock, M., Rodger, A. S., Dudeney, J. R., Baker, K. B., Newell, P. T., Greenwald, R. A., and Greenspan, M. E.: 1993. 'Observations of an Enhanced Convection Channel in the Cusp Ionosphere', *J. Geophys. Res.* **98**, 3767.
- Reiff, P. H., Hill, T. W., and Burch, J. L.: 1977. 'Solar Wind Plasma Injections at the Dayside Magnetospheric Cusp', *J. Geophys. Res.* **82**, 479.
- Rosenbauer, H., Grünwaldt, H., Montgomery, M. D., Paschmann, G., and Scopke, N.: 1975. 'Heos 2 Plasma Observations in the Distant Polar Magnetosphere: The Plasma Mantle', *J. Geophys. Res.* **80**, 2723.
- Ruohoniemi, J.M. Greenwald, R. A.: 1996. 'Statistical Patterns of High Latitude Convection Obtained from Goose Bay HF Radar Observations', *J. Geophys. Res.* **101**, 21743.
- Ruohoniemi, J. M., and Baker, K. B.: 1998. 'Large-scale Imaging of High Latitude Convection with Super Dual Auroral Radar Network HF Radar Observations', *J. Geophys. Res.* **103**, 20797.
- Sauvaud, J.-A., Barthe, H., Aoustin, C., Thocaven, J. J., Rouzaud, J., Penou, E., Popescu, D., Kovrazhkin, R. A., and Afanasiev, K. G.: 1998. 'The ION Experiment Onboard the Interball-Aurora Satellite: Initial Results on Velocity-dispersed Structures in the Cleft and Inside the Aurora Oval', *Ann. Geophys.* **16**, 1056.
- Shelley, E. G., Sharp, R. D., and Johnson, R. G.: 1976. 'He⁺⁺ and H⁺ Flux Measurements in the Day Side Cusp: Estimates of Convection Electric Field', *J. Geophys. Res.* **81**, 2363.
- Shelley, E. G., Ghielmetti, A. G., Balsiger, H., Black, R. K., Bowles, J. A., Bowman, R. P., Bratschi, O., Burch, J. L., Carlson, C. W., Coker, A. J., Drake, J. F., Fischer, J., Geiss, J., Johnstone, A., Kloza, D. L., Lennartsson, O. W., Magoncelli, A. L., Paschmann, G.,

- Peterson, W. K., Rosenbauer, H., Sanders, T. C., Steinacher, M., Walton, D. M., Whalen, B. A., and Young, D. T. : 1995. 'The Toroidal Imaging Mass-angle Spectrograph (TIMAS) for the Polar Mission', *Space Sci. Rev.* **71**, 497.
- Smith, E. J., Lockwood, M., and Cowley, S. W. H.: 1992. 'The Statistical Cusp: The Flux Transfer Event Model', *Planet. Space Sci.* **40**, 1251.
- Sonnerup, B.U.Ö, Paschmann, G., Papamastorakis, I., Sckopke, N., Haerendel, G., Bame, S. J., Asbridge, J. R., Gosling, J. T., and Russell, C. T.: 1981. 'Evidence for Magnetic Field Reconnection at the Earth's Magnetopause', *J. Geophys. Res.* **86**, 10049.
- Trattner, K. J., Fuselier, S. A., Peterson, W. K., Sauvaud, J.-A., Stenuit, H., and Dubouloz, N.: 1999. 'On Spatial and Temporal Structures in the Cusp', *J. Geophys. Res.* **104**, 28411.
- Trattner, K. J., Fuselier, S. A., Peterson, W. K., Boehm, M., Klumpar, D., Carlson, C. W., and Yeoman, T. K.: 2002a. 'Temporal Versus Spatial Interpretation of Cusp Ion Structures Observed by Two Spacecraft', *J. Geophys. Res.* **107**(A10), 1287doi: 10.1029/2001JA000181.
- Trattner, K. J., Fuselier, S. A., Peterson, W. K., and Carlson, C. W.: 2002b. 'Spatial Features Observed in the Cusp Under Steady Solar Wind Conditions', *J. Geophys. Res.* **107**(A10), 128810.1029/2001JA000262.
- Trattner, K. J., Fuselier, S. A., Yeoman, T. K., Korth, A., Fraenz, M., Mouikis, C., Kucharek, H., Kistler, L. M., Escoubet, C. P., Rème, H., Dandouras, I., Sauvaud, J. A., Bosqued, J. M., Klecker, B., Carlson, C., Phan, T., McFadden, J. P., Amata, E., and Eliasson, L.: 2003. 'Cusp Structures: Combining Multi-spacecraft Observations with Ground Based Observations', *Ann. Geophys.* **21**, 2031.
- Weiss, L. A., Reiff, P. H., Carlson, H. C., Weber, E. J., and Lockwood, M.: 1995. 'Flow-alignment Jets in the Magnetospheric Cusp: Results from the Geospace Environment Modeling Pilot program', *J. Geophys. Res.* **100**, 7649.
- Wing, S., Newell, P. T., and Rouhoniemi, J. M.: 2001. 'Double Cusp: Model Prediction and Observational Verification', *J. Geophys. Res.* **106**, 25571.